Proposal of a new simplified coulomb friction model applied to electrohydraulic servomechanisms

PROPOSAL OF A NEW SIMPLIFIED COULOMB FRICTION MODEL APPLIED TO ELECTROHYDRAULIC SERVOMECHANISMS

Matteo D. L. Dalla Vedova Francesco Di Fiore

Department of Mechanical and Aerospace Engineering, Politecnico di Torino

ABSTRACT

The design of electro-hydraulic servomechanisms characterized by high precision requirements generally needs adequate knowledge of its characteristics, and, in particular, of nonlinear phenomena. Among these, Coulomb's frictional forces acting on the mechanical elements in relative motion are critical to guarantee an implementation capable of respecting the accuracy requirements. The correct evaluation of this phenomenon allows understanding the behaviour of the physical system considered, to estimate its performance by implementing it in a simulation environment, and to design new devices taking into account the relative constraints. Accurate modelling and simulation of the considered system generally imply the use of high order dynamic models (typically, of second-order nonlinear or higher). However, under certain conditions, it is possible (and advisable) to simplify the mathematical structure of the numerical model, degrading it to a simple first-order, reducing its complexity and computational cost and, nevertheless, still obtaining results comparable with higher-order models. In this paper, the authors propose a new computational model capable of being implemented within these degraded numerical models, allowing them to simulate the main effects due to dry frictions (Coulomb's model). This first-order dynamic model is compared with the corresponding second-order ones to evaluate their performances in different scenarios.

Keywords: Coulomb, degraded model, dry friction, electrohydraulic actuator, numerical simulation

1 INTRODUCTION

The design of hydraulically powered flight controls for aerospace, typical high position accuracy servomechanisms, involves the deep knowledge of their behaviours, markedly affected by the Coulomb friction. The proper evaluation of the friction forces and torques is usually necessary when an accurate simulation of the servomechanisms' dynamic behaviour is requested, i.e. to perform a suitable design or reliable monitoring of the system itself.
As reported in [1], the simulation of the dynamic behaviours of these systems may require mathematical models capable of taking into account the usually unwanted effects of dry friction forces (or torques), which affect more or less all working conditions.
Besides, if the system is equipped with mechanical end-of-strokes, their effect must be adequately taken into account by the model itself, without compromising the correct simulation of dry friction. Generally, whichever actuators types are, the motion transmission consists of a certain number of shafts, gears, screws, ballscrews, epicyclical gears, and so on, neglecting driving belts and pulleys.
The motion transmission elements are generally affected by dry friction, which may give rise to reversible or irreversible behaviour of the whole system [2-3]. So, the potentially relevant effect of the dry friction on the dynamic behaviour of the mechanical system requires proper simulation models able to provide, at the same time, high computational accuracy, compactness, and efficiency. To this purpose, numerous numerical models are available in the literature [4] which, although with different fields of use and levels of detail, allows simulating frictional effects (e.g. Karnopp [5], Quinn [6], Borello [1], Dahl [7], LuGre [8], elasto-plastic [9-10], Leuven [11] or GMS friction models [12]).
It should be noted that, in general, these friction algorithms are integrated within larger numerical models able to provide a suitably detailed simulation of the dynamic response of the mechanical systems in question [13].
Usually, these models describe the main characteristics of the simulated on-board devices (e.g. electrohydraulic [14] or electromechanical actuators [15-16]) with a wealth of details, adopting non-linear mathematical models of a sufficiently high order and with a suitable number of degrees of freedom [17]. Therefore, accurate modelling of a considered mechatronic system generally implies the use of high order dynamic models (typically, of second-order nonlinear or higher). However, under certain conditions (widely explained in the following of this work), it is possible (and advisable) to simplify the mathematical structure of the numerical model, degrading it to a simple first-order. When the necessary conditions exist (i.e. one or more higher-order terms of the mathematical model are negligible), the degradation of the model allows reducing the complexity and computational cost of the entire algorithm. At the same time, it still guarantees comparable results with those provided by the higher-order models.

2 AIMS OF THE WORK

The main objective of this paper is to propose a novel numerical friction algorithm, derived from the one proposed by Prof. Borello in [1], but properly conceived to be applied to dynamic models degraded to a first-order mathematical formulation. For instance, referring to the electrohydraulic actuator (EHA) considered in this paper, a second-order non-linear dynamic model generally represents it [13]. However, if the inertial effects are negligible with respect to viscous and elastic ones, it is possible to eliminate inertial contribution, degrading the model to a more straightforward first order.
In this context, Coulomb friction has an essential effect on the real dynamic performances of highly accurate position servomechanisms. To carry out a correct design of the same, it is necessary to implement a new friction model capable of complying with the physical properties of the real phenomenon and, at the same time, able to be integrated into this first-order degraded model.

3 CONSIDERED EHA NUMERICAL TEST-BENCH

To test the new friction simulation algorithm for degraded dynamic systems, the authors developed a dedicated numerical test-bench representative of an electro-hydraulic actuator [13]. In this way, it was possible to test the actuation system in different operating conditions, compare the "nominal" EHA model with the corresponding first-order degraded one and, finally, evaluate the performance (and the applicability field) of the different models of friction considered therein (i.e. the classic algorithm that can be implemented in the complete dynamic system [1] and the proposed new friction model suitable for first-order degraded dynamic system).

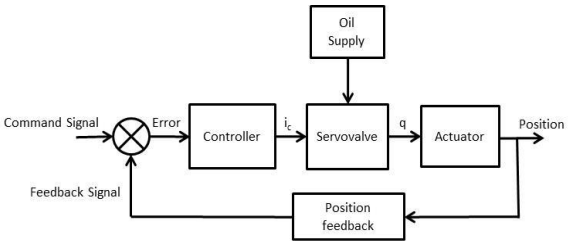

Figure 1 Block diagram of an electro-hydraulic position servo mechanism (EHA) [15].

3.1 REFERENCE SERVOMECHANISM DESCRIPTION

The servomechanism under exam is a typical position electrohydraulic servo control, used in primary and secondary aircraft's flight controls [15]. From a conceptual point of view, as shown in Figure 1, it can be schematically divided by the following subsystems:

- the controller subsystem made of control electronics and a servoamplifier; the control law implemented is PID (proportional-integrative-derivative);
- an electrohydraulic two stages servovalve;
- a hydraulic jack made of a symmetrical double acting linear cylinder affected by Coulomb friction;
- a position transducer (considered ideal, instantaneous and free to noise or errors) closing the control loop.

The full description of the EHA employed in the present work and its mathematical model are reported in [18].

The servomechanism considered belongs to the Fly-by-wire controls, excluding any type of mechanical interconnection between the control bar and the controlled aerodynamic surfaces [19]. The mechanical connections are replaced by a chain of transducers and sensors (potentiometers or encoders) which, by means of electric signals, send the position of the same to one or more computers that, after suitable processing, generate electrical impulses.

The signals produced are algebraically added to those deriving from the control ring, which instantaneously provides the position assumed by the moving surface, generating a signal proportional to the instantaneous position error of it. The implemented logic allows, using the error pulse, to actuate a control current which, thanks to the electrohydraulic servovalve (SVs), allows carrying out the actuation until the position assumed by the surface is the one originally sought by the pilot (tracking).

3.2 COMPLETE MODEL OF SERVOMECHANISM

As shown in Figure 2, the position error (*Err*) determined by the difference between the command (*Com*) generated by the pilot and the actual position (*XJ*) of the flight command, is converted by means of the PID control logic into a current input (*Cor*). This allows the first valve stage to be activated, resulting in a torque by the electric torque motor (expressed as a function of *Cor* and of the gain in torque *GM*). The generated torque allows the movement of the flapper (*XF*), explaining the dynamics of the valve second stage (modelled as a first-order system). As a consequence of the said torque, a displacement of the spool (*XS*) limited by a saturation block (hard stops) is generated.

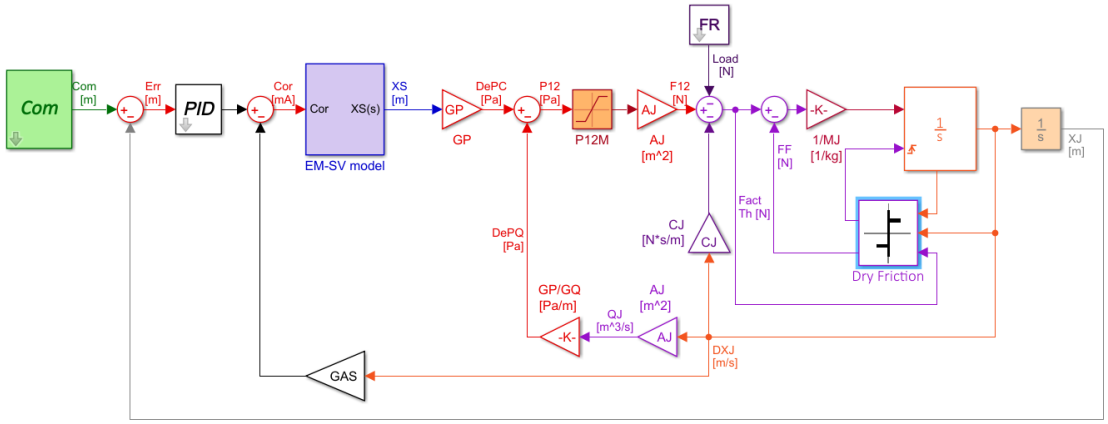

Figure 2 Simulink block diagram of the EHA equipped with the second-order dynamic model of the linear actuator.

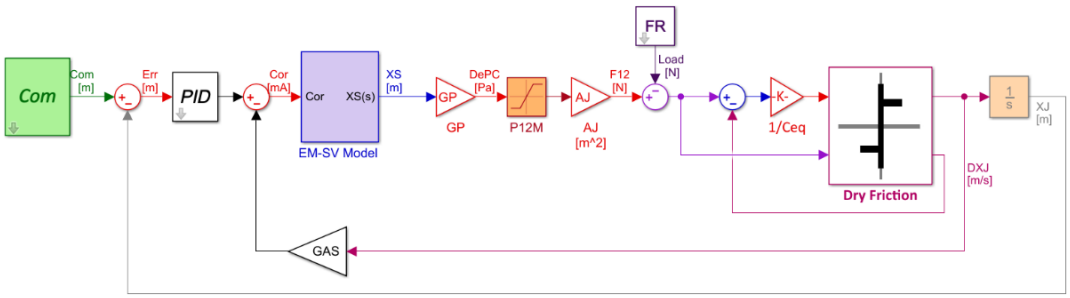

Figure 3 Simulink block diagram of the EHA equipped with the first-order dynamic model of the linear actuator.

The displacement *XS* allows to determine the differential pressure *P12* acting on the hydraulic piston suitably saturated. The two gains fluid dynamic valve model is implemented, by means that the differential pressure *P12* is determined as the difference between *XS* and the flows through the hydraulic jack *QJ* divided by *GQ* (flow gain), multiplied by *GP* (pressure gain). The differential pressure *P12* acting on the piston area (*AJ*) determines the pressure force *F12*. The net active force (*Act*) is determined by the comparison between *F12* and the other acting forces, considering the dry friction force (*FF*), the viscous force determined by the viscous coefficient (*CJ*), and the total load (*FR*) acting on the flight surface. The acceleration (*D2XJ*) is finally calculated as the ratio between the active force (Act) and the mass of the hydraulic jack (*MJ*). Its integration gives the velocity (*DXJ*), determining the viscous term and the working flow *QJ* above discussed. The integration of the velocity gives the instantaneous jack position (*XJ*) that allows closing the feedback ring (considering the position transducer as ideal).

4 DEGRADATION OF THE EHA DYNAMIC MODEL

The dynamics of the linear actuator (i.e. the hydraulic jack) that equips the EHA adopted as a numerical test-bench in this article, in a nutshell, can be associated with a typical mechanical mass-spring-damper system. In other words, referring to the coefficients introduced in the previous chapter, it is possible to obtain the mathematical model of the actuator through the equation of equilibrium at the linear translation (in direction XJ) of the forces acting on the jack:

$$MJ \cdot D2XJ + CJ \cdot DXJ = F12 - FR - FF \qquad (1)$$

where, in linearity conditions (i.e. when the differential pressure *P12* is, in modulus, lower than its saturation value *P12M*), the pressure force *F12* can be expressed as:

$$F12 = (DePC - DePQ) \cdot AJ \qquad (2)$$

$$DePC = XS \cdot GP \qquad (3)$$

$$DePQ = GP/GQ \cdot AJ \cdot DXJ \qquad (4)$$

If the inertial term $MJ \cdot D2XJ$ is negligible when compared with the other forces shown in Eq. (1), the degradation of the system is possible. In case of small masses of the hydraulic jack (or, in general, when the inertial term $MJ \cdot D2XJ$ is globally negligible), the simulation model can be modified as shown in Figure 3. It is computed an equivalent damping coefficient (C_{eq}), calculated as the sum of the damping coefficient (*CJ*) and the term bound to the fluid dynamic valve model ($GP/GQ \cdot AJ^2$). In this case, given that the overall inertia of the system is neglected, the actual value of the actuation speed *DXJ* is directly proportional to the net force acting on the jack.
So, in the case of a dynamic model degraded to first-order, *DXJ* changes instantaneously with the net acting force (*Act*)
The instantaneous value of *DXJ* is obtained as the ratio between the net force *Act* acting on the piston (that, referring to Figure 3, is expressed as *Act=F12–FR–FF*) and the equivalent damping coefficient C_{eq}. As already for the second-order model, the instantaneous value of the position of the jack *XJ* can be obtained by the temporal integration of the corresponding value of the *DXJ* actuation speed.

4.1 ADVANTAGES, DISADVANTAGES, AND LIMITS OF APPLICABILITY OF DEGRADED MODELS

Matlab-Simulink calculates the dynamic response of the simulated system using an approximate numerical resolution [20]. In this specific case, to integrate the differential equations of the mathematical model of the system (and, therefore, calculate the dynamic response), a fixed-step solver based on the Euler method was adopted [21].

The definition of the integration step DT used in Euler's method is carried out taking into account the vibrational behavior of the analyzed mechanical system. Considering the analysis of the dynamic response of mechanical systems with mass, it is important to examine mechanical vibrations, that is the oscillation of the structure around the equilibrium position. The mechanical oscillations of a second order system (such as the one in question) are characterized by some parameters including the natural frequency of the non-damped system, the critical dumping and the not dimensional dumping (the formulation of which is shown below). If the mass of the hydraulic jack is reduced, the natural frequency of the second order system increases. This entails the need to reduce the integration step, with an increase in the computational cost, in order to obtain a reliable simulation analysis from the point of view of the results. However, as the mass decreases, the critical damping of the system increases. Overall, the system increases the number of oscillations in the time unit but is more dampened. This turns out to be a paradox given that a model whose simulation response is over-damped requires a smaller integration step than the same model with higher critical damping. Hence the possibility of neglecting the inertial term and consequently approximating the response of a second order system to a first order. This allows to overcome the numerical problems (limit cycle) that arise in the application of an integration step less than a certain threshold. However, considering the application of an oscillatory forcing such that the natural frequency of the system increases considerably, the pulsation of the system will increase and consequently the acceleration of the system will increase. This makes it impossible to neglect the inertial term $MJ \cdot D2XJ$ even in the presence of a contained mass. The necessary requirements to be able to degrade the model are summarized as follows:

- Hydraulic jack mass defined below a certain threshold which will depend on the characteristics of the servomechanism in question.
- Operating frequency range included within a suitable band defined by the vibrational characteristics of the mechanical system in question.

5 CLASSICAL COULOMB FRICTION MODELS

In general, dry friction is generated between two moving mechanical elements. It can be considered as a force opposed to motion whose direction of application depends on the direction of the velocity vector. This concept is represented by the Coulomb friction model [22], which can be summarized in the following points:

- in static conditions, when the velocity vector is zero, the frictional force (*FF*) is an equal and opposite vector to the applied moving force (*Act Th*) until this assumes the value of the limit static frictional force value (*FSJ*) (incipient motion condition);
- in dynamic conditions, when the velocity is not zero, the friction force assumes a modulus equal to the dynamic friction force (*FDJ*) and the vector opposes the motion.

The classical Coulomb friction model can be generally represented by the following relationships, taking into account the difference between sticking and slipping conditions:

$$FF = \begin{cases} Act\ Th & IF\ \ v = 0 \wedge |Act\ Th| \leq FSJ \\ FSJ \cdot sign(Act\ Th) & IF\ \ v = 0 \wedge |Act\ Th| > FSJ \\ FDJ \cdot sign(v) & IF\ \ v \neq 0 \end{cases} \quad (5)$$

where *FSJ* and *FDJ* represent the friction force in sticking and slipping conditions respectively, *Act Th* is the active force and *v* represents the relative slipping velocity.

This strongly non-linear relationship (discontinuous and undefined in null velocity conditions) entails a difficulty in the numerical implementation of the same in order to describe the system in a simulation environment.

It should be noted that the model proposed in this article is characterized by a discontinuous friction algorithm, so that the discontinuous friction force in sticking regime is considered and presents an action aimed to balancing the other forces in order to keep the speed null (until the friction force does not reach the maximum value equal to the static friction force). The algorithm allows a distinction to be made in four behaviours of a mechanical element in the presence of dry friction:

- An initially stopped mechanical element must remain in a stick condition.
- An initially stopped mechanical element must break away.
- An initially moving mechanical element that must remain in motion.
- An initially moving mechanical element that must stop.

The model, therefore, allows correctly evaluate the sign of the friction force as a function of the actuation rate sense, to distinguish the static conditions from the dynamic ones, to evaluate the possible stop of a mechanical element initially in motion, to keep it correctly in conditions of grip or considering restarting the movement. The analysis of the behaviour of a servomechanism requires its description by means of a higher order model.

The authors, as shown in Chapter 3, consider a second order model representative of the servomechanism in which the previously discussed friction algorithm is implemented [13-14].
However, since high accuracy and reduced computational costs (CPU, RAM) are required in preliminary design and monitoring phase, fast models which are able to highlight the peculiar aspects of the system by reducing calculation times are needed. This is sometimes incompatible with models with high descriptive accuracy (higher order).
The authors aim is to examine the possibility of degrading the model to a first order, in the hypothesis that the mass-dependent inertial term was negligible, and to demonstrate the ability to evaluate the key aspects of the system by reducing computational costs associated with the accurate simulation of the same.

5.1 BORELLO'S DRY FRICTION MODEL AND RELATED ALGORITHM

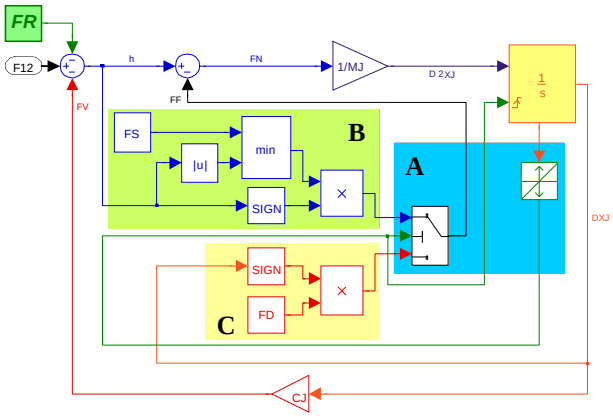

Figure 4 Block diagram of the Matlab- Simulink discrete friction force algorithm proposed by Borello [1].

Borello's dry friction computational algorithm, from which the authors developed the new method applied to dynamic systems degraded to first-order numerical models, was initially implemented in the FORTRAN environment (according to Eqs. 6-12), and, subsequently, it has also been developed in Matlab-Simulink language, as shown in Figure 4, and widely described in [23].

$$Act\ Th = F12 - FR - FV \tag{6}$$

$$FF = \mathrm{SIGN}(FDJ, DXJ) \tag{7}$$

$$IF(DXJ.EQ.0)\quad FF = \mathrm{MIN}(\mathrm{MAX}(-FSJ, Act\ Th), FSJ) \tag{8}$$

$$D2XJ = (ActTh - FF)/MJ \tag{9}$$

$$Old = DXJ \tag{10}$$

$$DXJ = DXJ + D2XJ \cdot DT \tag{11}$$

$$IF(Old \cdot DXJ.LT.0)\quad DXJ = 0 \tag{12}$$

5.2 NEW DRY FRICTION ALGORITHM APPLIED TO SECOND-ORDER DYNAMIC MODELS

The proposed dry friction algorithm, implemented starting from the Borello's model, has been developed in Matlab-Simulink language (one of the most commonly used languages in engineering applications) and its logic is schematically shown in the block diagram of Figure 5.

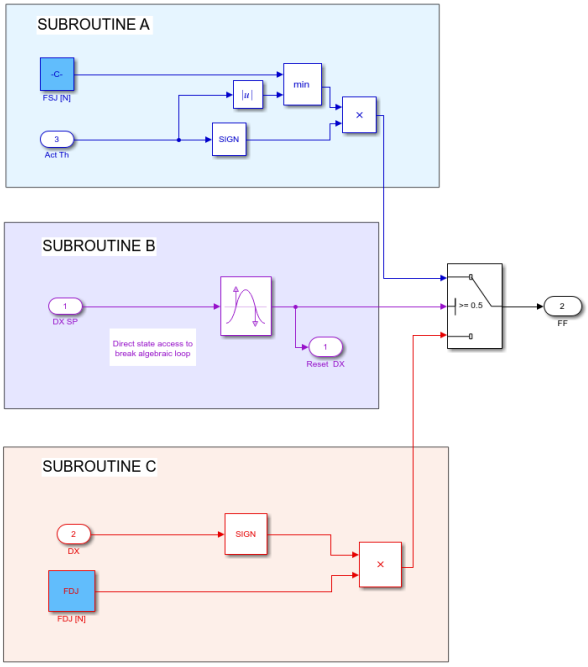

Figure 5 Block diagram of the proposed friction algorithm applied to second-order dynamic models.

The proposed friction model was implemented in the Simulink block diagram of the EHA (Figure 2) within the subsystem called "*Dry Friction*". Its block diagram can be summarized by the following computational routine:

$$reset\ DXJ = pass(DXJ\ SP) \quad (13)$$

$$IF\ Pass(DXJ\ SP) = 1 \quad (14)$$

$$THEN\ FF = sign(Act\ Th) \cdot min(|Act\ Th|, FSJ) \quad (15)$$

$$ELSE\ sign(DXJ) \cdot FDJ \quad (16)$$

$$END\ IF \quad (17)$$

The actuation speed *DXJ* of the hydraulic jack is computed starting from the Boolean signal coming from the "*Hit-Crossing*" block defined by the function pass (*DXJ SP*), where *DXJ SP* is the instantaneous speed output from the integrator state port. The next rows of the meta code reported in Eqs. (13-17) describe the discrimination of the adhesion or slipping condition by means of an *IF* and *ELSE* algorithm. The distinction between the two regimes is defined by the balance between the resultant of the active forces and the frictional force. When the resultant applied exceeds the adhesion force, the transition from static to dynamic occurs. If the Boolean signal is equal to the unit (Eq. 14), then the friction force is computed in the static condition. *FF* is equal to the minimum between the modulus of active forces and the static friction force value multiplied by the sign of the friction forces (Eq. 15). Vice versa, *FF* is computed as the product of the dynamic friction force and the sign of speed in slipping condition (Eq. 16). The friction force thus calculated is subtracted from the resultant of the active forces allowing the determination the jack acceleration.

I analogy with [1], the proposed model is capable of: providing the sign of the frictional force in relation to the sign of the speed; to distinguish the conditions of adhesion from those of motion; evaluate the starting and stopping of the considered mechanical element; keep the mechanical element considered in the stop or motion state.

The peculiarity of the model resides in the fact that the stop is imposed if the speed value goes through zero. Stopping in the event of a speed reversal can be expressed as:

$$v(t\_(i+1)) = 0\ if\ v(t\_(i+1)) \cdot v(t\_i) \leq 0 \quad (18)$$

At the next step, if the value of the external force exceeds the static frictional force, the system would still be able to restart. In conditions of adherence, the friction force is considered equal and opposite to the sum of the active forces; however the frictional force cannot exceed the static frictional force *FSJ* value as specified in Eq. (15) of the computational routine and in *Subroutine A* of the simulink scheme of Figure 5. The result is an *FF* equal to *FSJ* in the opposite direction of *Act Th*.

When the condition for which *Act Th* is greater than *FSJ* occurs, the slipping condition is determined in accordance with Eqs. (15-16); the *DXJ* value is different from zero and will be the input of the next computational step. On the other hand, if the adhesion condition persists, that is *Act Th* minor than *FSJ*, the *DXJ* value will be kept null. In slipping condition, the frictional force assumes a value equal to *FDJ* in accordance with Eq. (16) and *Subroutine C*. The result is an *FF* equal to the *FDJ* in the opposite direction as *Act Th*. The authors' Simulink algorithm implements the aforesaid breakaway detection by means of a "*Switch*" block. The switching condition is given, as shown in *Subroutine B*, by the instantaneous value of *DXJ* coming from the integrator state port, allowing the selection between sticking and slipping condition by means of a hit crossing block and the correct computation of *FF*.
The dynamic response of the system is simulated by numerical integration performed with the Euler method:

$$DXJ = DXJ + D2XJ \cdot DT \qquad (19)$$

The value assumed by *DXJ* at each integration step represents the input of the Simulink model just discussed; when there is an inversion of the sign of speed in the current computational step, that is a passage in the zero speed condition, the speed must be imposed null.
In the following integration step, the condition of adherence will be imposed and, if *Act Th* is lower than *FSJ*, it will be maintained; vice versa, if $|Act\ Th|$ is higher than *FSJ*, the slipping condition will be determined.

6 PROPOSED DRY ALGORITHM APPLIED TO DEGRADED FIRST-ORDER DYNAMIC MODELS

In case of degraded EHA model, as shown in Figure 6, the authors' friction algorithm is modified as follows:

- as indicated in the previous paragraph, it is possible to determine from the balance of forces (considering negligible the inertial term $MJ \cdot D2X$) the actuation speed (*DX Th*) which constitutes the input of the friction algorithm together with *Act Th*.
- The speed computation at the current integration step (*DX*) is carried out by means of a memory block (as shown in Figure 7), which allows to break the algebraic loop which otherwise would occur with a simple feedback.
- The reset signal (named *Reset DX*), which determines the switch condition between adhesion and slipping, is calculated starting from the aforesaid speed *DX Th*.

Act Th and the actuation speed *DX Th* are in input to the friction block. The switch block activation condition is defined by the *Reset DX* signal. As shown in *Figure 7*, the instantaneous value of the actuation speed *DX Th* is calculated by comparing it with the real speed *DX*, calculated in the previous simulated instant. If the product of the two speeds is positive (i.e. when they are both non-zero and with concordant sign), the logic bloc gives an output equal to 1 and, then, *DX* = *DX Th*. Vice versa, if one of the two speeds is null or they have opposite sign, the instantaneous *DX* speed provided downstream of the "*Multiplier*" block is set to zero. In this way, if the speed shows a sign inversion, a null *DX* output speed is selected.
The "*Memory*" block positioned on the *DX* feedback branch, supplying the speed value received as input at the previous instant as output, introduces a delay equal to an integration step *DT* in the ring mentioned above. This solution allows breaking the algebraic loop related to the *DX* counteraction ring and, so, to avoid numerical issues.

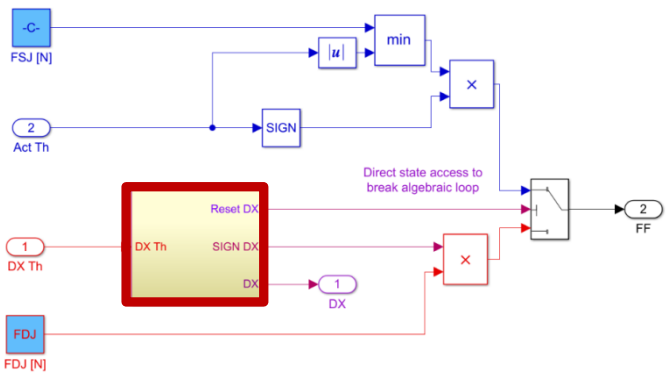

Figure 6 Block diagram of the proposed friction algorithm applied to degrader first-order dynamic models.

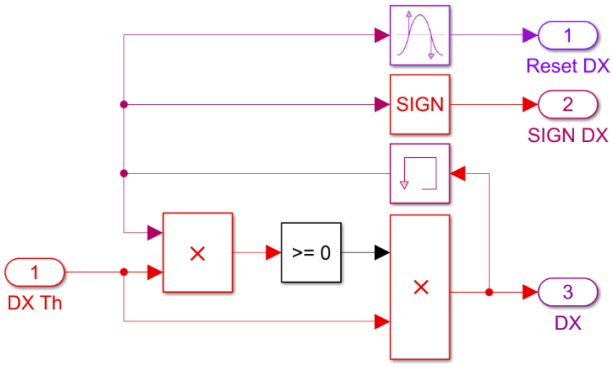

Figure 7 Detail of the "*Reset DX*" subsystem of Figure 6.

An algebraic loop occurs when a signal loop exists with only direct feedthrough blocks within the loop, which means that Simulink needs the block's input signal value to calculate its output in the current time phase. Such a signal circuit creates a circular dependence of the outputs and inputs of the blocks at the same time step. This translates into an algebraic equation that must be solved at each stage, adding computational costs to the simulation of the impossibility of computation. The *SIGN DX* signal provides the sign of the *DX* speed calculated in a given simulation instant. It is calculated using a Simulink block of type "*SIGN*" that provides an output equal to 1 if the speed is positive and -1 if the speed is negative. The *Reset DX* signal is finally determined by a "*Hit-Crossing*" block, detecting when the input signal crosses the zero value. If the passage from zero takes place, then the output will be equal to 1, calculating a *FF* as static friction (i.e. related to adherence conditions). Otherwise, *FF* is associated with sliding conditions and, therefore, is obtained using the dynamic model. The algorithm thus computed does not require the instantaneous speed value coming from the state port of the acceleration integrator. In fact, the application of the friction algorithm described for the second order system was impossible due to the simplification inherent in the degraded model. By reducing the degree of the physical system, the corresponding Simulink model presents only the speed integrator, not allowing the determination of the speed computed at the current step before its declaration by the integrator. The use of the memory block, therefore, allows overcoming the problem in the manner described previously. In this way, it is possible to apply the friction model to the degraded system and compare it with the second-order system in the following chapters.

7 ANALYSIS OF THE NUMERICAL RESULTS

To evaluate the performance of the proposed friction algorithm (applied to degraded-order dynamic model), we compared the time responses generated by the detailed numerical model (equipped with a second-order dynamic model) with those obtained with the actuator model degraded to the first order. For shortness, in this paper are reported only some explanatory cases, suitable to put in evidence the main models' peculiarities; interested readers can directly test the models illustrated downloading them online from [XXX]. In Figure 8, the response of the high-order system was tested by varying the mass of the actuator from 0.1 kg (purple line) to 1000 kg (yellow) based on a logarithmic progression of the system inertia. Figure 8 shows the models response for a step command of 0.2 m, applied at time = 0.005 seconds. Note that, when the inertia decreases, the dynamic response provided by the second-order models pack closer to those of the first order, both in the start-up transient and in stationary conditions (e.g. static positioning error due to friction). In this case, the response of the first-order model cannot be identified in the figure because it tends to overlap almost entirely with that of the second-order system with very low inertia (MJ = 0.1 kg).

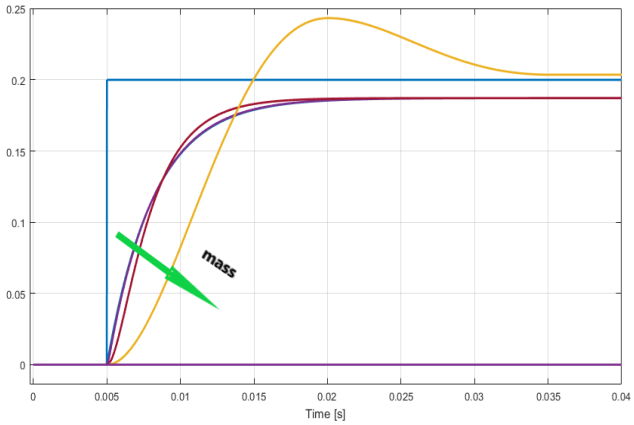

Figure 8 EHA response for a step command of 0.2 m. Comparison, as the actuator mass MJ varies, between the second-order model and the corresponding first-order degraded one. The mass MJ varies from 0.1 kg (purple line) to 1000 kg (yellow line) in a logarithmic progression.

As reported above, if the inertia is negligible, the dynamic response of the first-order model of the EHA (Figure 9) is substantially identical to that generated by a second-order system (Figure 10). Obviously, as the mass of the system increases (Figures 12 and 13), the trend of the simulated position XJ (red curve) will begin to deviate from the equivalent response of the degraded system. Note also how, at least for reduced masses (Figures 10-11), the trend of the speed transient (yellow line) and the value of the steady-state error (i.e. the difference between the command - blue line - and the position of the actuator - red line) basically follow what simulated by the degraded model (Figure 9)

Vice versa, considering higher masses (100 kg), the break-away speed transient becomes more evident (Figure 12). Its position time- response shows a significantly increasing delay compared to the first-order system because, in this case, inertial reactions are no longer negligible.

When the inertial term becomes predominant (e.g. in the case shown in Figure 13, having mass MJ = 1000 kg), there is a reduction in the stability margin of the system associated with the onset of oscillatory phenomena. In this case, of course, the first-order degraded model falls short as it is not capable of simulating the oscillatory dynamics of an under-damped system. In Figures 14-18, the response of the two systems to a position ramp command is considered.

The dynamic response of the simulated systems is characterized by a break-away transient (related to the slope of the command input and the dynamic characteristics of the different models), followed by a section in which the EHA moves at a constant speed (equal to the slope of the commanded ramp) along a straight path with a slope equal to that of the command. Note the peak of actuation speed following the break-away is caused by the momentary imbalance between the actuation force and the friction force. As already explained in chapters 5 and 6, this is because the transition from the adhesion to the sliding condition is a non-linear phenomenon in which the friction force markedly reduces (according to Eq. 5).

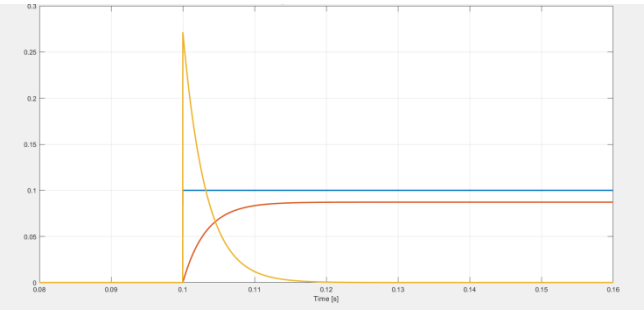

Figure 9 EHA first-order degraded model.

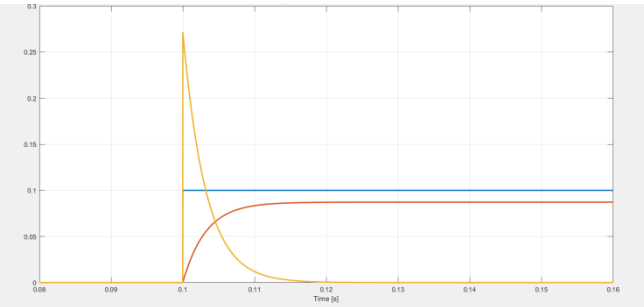

Figure 10 EHA second-order model – MJ = 0.1 [kg].

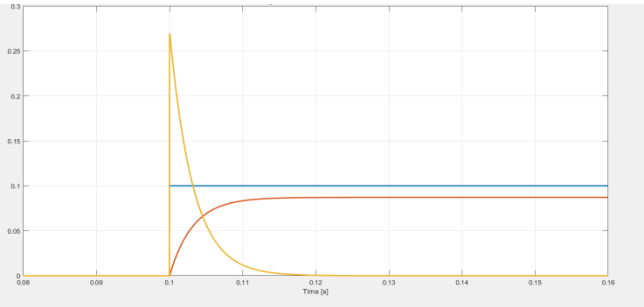

Figure 11 EHA second-order model – MJ = 1 [kg].

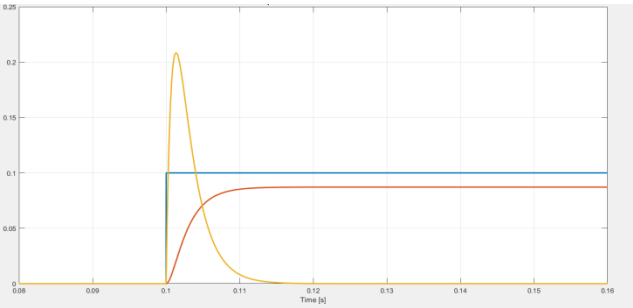

Figure 12 EHA second-order model – MJ = 100 [kg].

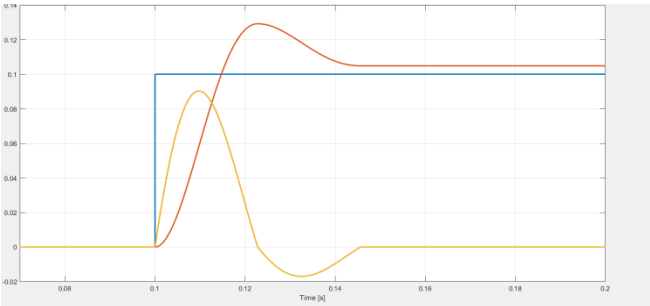

Figure 13 EHA second-order model – MJ = 1000 [kg].

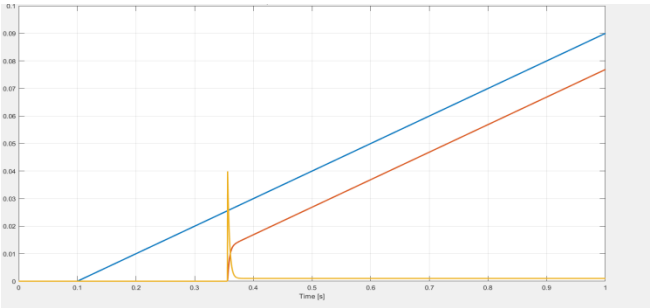

Figure 14 EHA first-order degraded model.

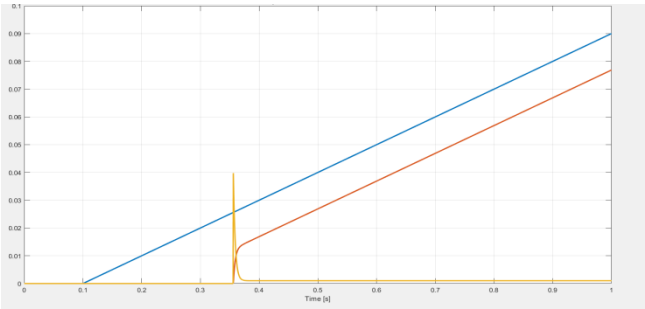

Figure 15 EHA second-order model – MJ = 0.1 [kg].

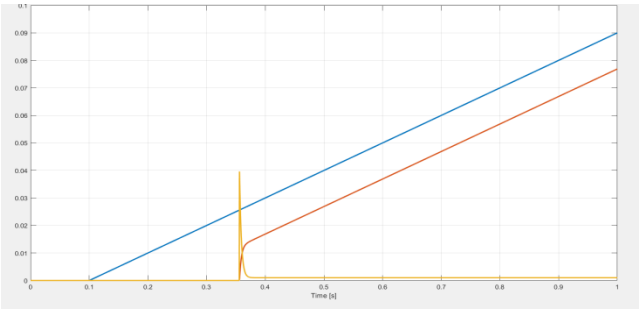

Figure 16 EHA second-order model – MJ = 1 [kg].

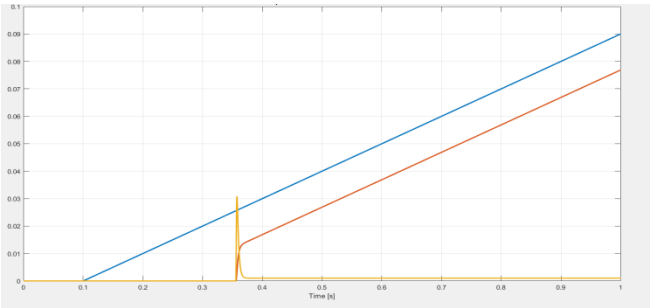

Figure 17 EHA second-order model – MJ = 100 [kg].

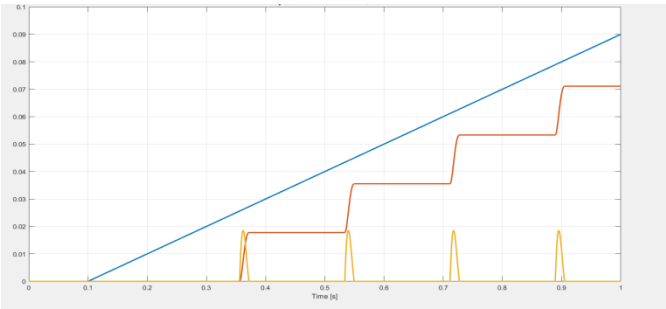

Figure 18 EHA second-order model – MJ = 1000 [kg].

As the mass involved increases, the peak takes on lower values since the accelerations connected to it are less.
In the case of very high inertia (markedly undercut systems and a sufficiently high ramp slope), the second-order system generates a stick-slip phenomenon [18, 23].

8 CONCLUSIONS

The simulations show the accuracy of the proposed algorithm taking into account the effects of dry friction on the behaviour of the actuators. It should be noted the proposed models can correctly describe the dynamic/static behaviour of the considered on-board electrohydraulic actuators for primary flight controls. The degraded first-order model is still able to simulate with suitable precision the dynamic response of the considered EHA taking into account the effects due

to several nonlinear phenomena (i.e. friction force on the mechanical transmission, pressure saturation of the hydraulic pressure regulated by the EHA servo valve, ends-of-travels acting on the jack stroke).
The simulations prove that the first-order model is an excellent choice to describe servomechanisms characterized by low inertia (i.e. the inertial term of the mathematical model is negligible compared to viscous or elastic ones), but it is not recommended for higher-inertia systems. Furthermore, for these dynamic systems, the second-order model can be used with greater temporal discretization due to the low speed and the frequencies at which they work, and therefore numerical problems should not occur.

ACKNOWLEDGEMENTS

The authors would like to thank Prof. Lorenzo Borello for his precious teachings and his essential contribution to the conception and development of these research topics.

LIST OF SYMBOLS

Act Th	sum of active forces	$[N]$
AJ	piston active area	$[m^2]$
CJ	dimensional viscous coefficient	$[Ns/m]$
Com	command signal	$[m]$
Cor	servovalve piloting current	$[mA]$
Err	position error	$[m]$
D2XJ	acceleration of the piston rod	$[m/s^2]$
DXJ	velocity of the piston rod	$[m/s]$
F12	hydraulic force acting on piston	$[N]$
FR	external load acting on piston rod	$[N]$
FV	viscus force acting on piston rod	$[N]$
GP	pressure gain of the SV spool	$[Pa/m]$
GQ	flow gain of the the SV spool	$[m^2/s]$
MJ	equivalent mass of the actuator	$[kg]$
P12	hydraulic differential pressure	$[Pa]$
QJ	working flow	$[m^3/s]$
XF	valve first -stage displacement	$[m]$
XS	valve second-stage displacement	$[m]$
XJ	aerodynamic surface position	$[m]$

REFERENCES

[1] Borello L., Dalla Vedova M.D.L., A dry friction model and robust computational algorithm for reversible or irreversible motion transmissions. *International Journal of Mechanics and Control (JoMaC)*, Vol. 13, No. 02, pp. 37-48, December 2012. ISSN: 1590-8844.

[2] Borello L., Villero G., Dalla Vedova M.D.L., New asymmetry monitoring techniques: effects on attitude control. *Aerospace Science and Technology*, Vol. 13, No. 8, pp. 475-487, 2009.

[3] Borello L., Villero G., Dalla Vedova M.D.L., Flap failure and aircraft controllability: Developments in asymmetry monitoring techniques. *Journal of Mechanical Science and Technology*, Vol. 28, No. 11, pp. 4593-4603, 2014. ISSN: 1738-494X.

[4] Liu Y.F., Li J., Zhang Z.M., Hu X.H., Zhang W.J., Experimental comparison of five friction models on the same test-bed of the micro stick-slip motion system. Mechanical Sciences, Vol. 6, pp. 15-28, 2015.

[5] Karnopp D., Computer simulation of stick-slip friction in mechanical dynamic systems. *Journal of Dynamic Systems, Measurement, and Control*, Vol. 107, 1985.

[6] Quinn D., A new regularization of Coulomb friction. *Journal of Vibration and Acoustics*, Vol. 126, No. 3, pp. 391-397, 2004.

[7] Dahl P.R., *A solid friction model*. Technical Report Tor-0158(3107-18)-1, The Aerospace Corporation, El Segundo, CA, 1968.

[8] Canudas de Wit C., Olsson H., Åström K.J., Lischinsky P., A New Model for Control of Systems with Friction. *IEEE Transactions on Automatic Control.*, Vol. 40, pp. 419-425, 1995.

[9] Kikuuwe R., Takesue N., Sano A., Mochiyama H., Fujimoto H., Fixed-step friction simulation: from classical coulomb model to modern continuous models. *International Conference on Intelligent Robots and Systems IEEE/RSJ 2005*, pp. 3910-3917, June 2005.

[10] Dupont P., Armstrong B., Hayward V., Elasto-plastic friction model: contact compliance and stiction. *Proceedings of the American Control Conference*, Vol. 2, pp. 1072-1077, June 2000.

[11] Swevers J., Al-Bender F., Ganseman C.G., Prajogo T., An integrated friction model structure with improved presliding behaviour for accurate friction compensation. *IEEE Transactions on Automatic Control*, Vol. 45, pp. 675-686, 2000.

[12] Lampaert V., Swevers J., Al-Bender F., Modification of the Leuven integrated friction model structure. *IEEE Transactions on Automatic Control*, Vol. 47, pp. 683-687, 2002.

[13] Borello L., Villero G., Flap control system actuators: mathematical and computational model for dynamic simulation, *European Congress on Computational Methods in Applied Sciences and Engineering ECCOMAS 2000*, Barcellona, Spain, 2000.

[14] Borello L., Dalla Vedova M.D.L., Jacazio G., Sorli M., A prognostic model for electrohydraulic servovalves. *Annual Conference of the Prognostics and Health Management Society, PHM 2009*, San Diego, CA, 2009.

[15] Dalla Vedova M.D.L., Maggiore P., Pace L., Proposal of prognostic parametric method applied to an electrohydraulic servomechanism affected by multiple failures. *WSEAS Transactions on Environment and Development*, Vol. 10, pp. 478-490, 2014.

[16] Dalla Vedova M.D.L, Germanà A., Maggiore P., Proposal of a new simulated annealing model-based fault identification technique applied to flight control EM actuators. *Risk, Reliability and Safety: Innovating Theory and Practice: Proceedings of ESREL 2016*, Glasgow, UK, 25-29 September 2016, pp. 313-321. ISBN: 978-1-138029-97-2.

[17] Belmonte D., Dalla Vedova M.D.L., Maggiore P., Electromechanical servomechanisms affected by motor static eccentricity: Proposal of fault evaluation algorithm based on spectral analysis techniques. *Safety and Reliability of Complex Engineered Systems - Proceedings of the 25th European Safety and Reliability Conference, ESREL 2015*, pp. 2365-2372, 2015.

[18] Borello L., Maggiore P., Dalla Vedova M.D.L., Alimhillaj P., Dry fiction acting on hydraulic motors and control valves: dynamic behavior of flight controls. *XX Congr.Nazionale AIDAA*, Milano, 2009.

[19] Moir I., Seabridge A., Aircraft Systems: Mechanical, Electrical, and Avionics Subsystems Integration. 3rd edition, Wiley, August 2011.

[20] Klee H., Allen R., Simulation of dynamic systems with MATLAB and Simulink. Boca Raton, 2018.

[21] Biswas B.N., Chatterjee S., Mukherjee S., Pal S., A discussion on Euler method: a review. *Electronic Journal of Mathematical Analysis and Applications*, Vol. 1, No. 2, pp. 294-317, July 2013.

[22] Popova E., Popov V.L., The research works of Coulomb and Amontons and generalized laws of friction. *Friction*, Vol. 3, No. 2, pp. 183-190, 2015.

[23] Borello L., Maggiore P., Villero G., Dalla Vedova M.D.L., A comparison between dry friction discontinuous computational algorithms. *27th Congress of the International Council of the Aeronautical Sciences, ICAS 2010*, Vol. 5, pp. 3750-3759, 2010.

[24] Dalla Vedova M.D.L., Simulink_Files JoMaC21A.zip, *https://www.dropbox.com/s/tg11dogi74h7dx6/Simulink_Files%20JoMaC21A.zip?dl=0*.